



## Operating characteristics of aqueous magnetite electrochemical capacitors

S-Y. WANG and N-L. WU\*

Department of Chemical Engineering, National Taiwan University, Taipei 106, Taiwan, R.O.C.

(\*author for correspondence, e-mail: nlw001@ccms.ntu.edu.tw)

Received 28 October 2003; accepted in revised form 18 January 2003

**Key words:** electrochemical capacitor, leakage current, magnetite, pseudocapacitance, self-discharge

### Abstract

Operating characteristics, including capacitance, leakage current, operating potential range, cycling stability and open-circuit self-discharge behaviours, of the magnetite ( $\text{Fe}_3\text{O}_4$ ) supercapacitor, containing 10 wt % carbon black as conductive additive, in aqueous electrolytes of  $\text{Na}_2\text{SO}_3$ ,  $\text{KOH}$  and  $\text{Na}_2\text{SO}_4$  were investigated. Although the capacitance of the oxide was found to depend heavily on electrolyte composition, the self-discharge mechanism in these electrolytes appeared to be the same. Reduction in the dissolved oxygen content (DOC) of the electrolyte reduced the leakage current and profoundly improved the cycling stability. In particular,  $\text{Na}_2\text{SO}_3(\text{aq})$  gives the highest capacitance, nearly  $30 \text{ F (g-Fe}_3\text{O}_4)^{-1}$  or  $80 \mu\text{F cm}^{-2}$  of actual surface area, with an operation range of 1.1 V based on a leakage current less than  $0.1 \text{ mA F}^{-1}$ , and the electrode showed no deterioration after  $10^4$  cycles under a  $\text{DOC} < 0.1 \text{ ppm}$ .

### 1. Introduction

Regular electrical double layer (EDL) capacitance arises from potential-dependence of the surface density of charges stored electrostatically (i.e., nonfaradaically) at the interfaces of capacitor electrodes [1–4]. EDL electrochemical capacitors are complemented by capacitors based on the pseudocapacitance (PC), which take places in either electrosorption processes or redox reactions at electrode surfaces of materials, such as  $\text{RuO}_2$ ,  $\text{IrO}_2$ ,  $\text{MoN}$ ,  $\text{Co}_3\text{O}_4$ , some carbon compounds and other metal oxides [5–14]. PC can be 10 to 100 times greater than the EDL capacitance per unit true area of the electrode material. In particular, amorphous hydrated  $\text{RuO}_2$  has attracted considerable attention as it shows a high capacitance of over  $700 \text{ F g}^{-1}$  and excellent cyclability [15]. However,  $\text{RuO}_2$  is too expensive to be commercially attractive. Therefore, searching for less expensive PC electrode material has been a major subject in supercapacitor research [10, 12, 16, 17].

We have previously characterized the basic capacitive behaviours of magnetite in several aqueous electrolytes, including aqueous solutions of  $\text{Na}_2\text{SO}_4$ ,  $\text{NaCl}$ ,  $\text{KOH}$ ,  $\text{Na}_3\text{PO}_4$ , and  $\text{Na}_2\text{SO}_3$ , and three categories were observed. First, neutral electrolytes, including  $\text{Na}_2\text{SO}_4(\text{aq})$  and  $\text{NaCl}(\text{aq})$ , gave capacitances ( $3\text{--}5 \text{ F g}^{-1}$ ) close to the space-charge capacitance of the oxide. Secondly, the strong basic electrolytes, including  $\text{KOH}(\text{aq})$  and  $\text{Na}_3\text{-PO}_4(\text{aq})$  gave rise to a higher capacitances ( $5\text{--}7 \text{ F g}^{-1}$ ) which can, in part, be attributed to pseudocapacitance involving  $\text{OH}^-$ . Finally,  $\text{Na}_2\text{SO}_3(\text{aq})$  gave the highest

capacitance, which, depending heavily on dispersion of magnetite crystallites on the conductive matrix, range from about 30 to  $510 \text{ F g}^{-1}$  [18]. In the present study, several operating characteristics, including leakage current, operating potential range, cycling stability and open-circuit self-discharge behaviours, of the oxide electrode in these electrolytes were investigated. Aqueous solutions of  $\text{Na}_2\text{SO}_3$ ,  $\text{KOH}$  and  $\text{Na}_2\text{SO}_4$  were selected respectively as the representatives for the three categories.

### 2. Experimental details

Magnetite ( $\text{Fe}_3\text{O}_4$ ) crystallites with an average crystallite size of 14 nm, as determined by X-ray diffraction (XRD), were produced via an electrocoagulation process illustrated by Tsouris et al. [19]. The apparatus comprised a container holding an electrolytic solution of  $0.04 \text{ M NaCl}(\text{aq})$  and a power supply applying a voltage (30 V) to a pair of carbon steel plates for a period of time that was sufficient to produce high-purity magnetite crystallites. The resulted magnetite particles were finally washed with deionized water and dried at  $40 \text{ }^\circ\text{C}$  in vacuum.

It has previously [18] been found that, due to limited conductivity of magnetite, it is necessary to combine the oxide with conductive additives in order to obtain significant capacitance. In the present study, composite electrodes were prepared by mixing the magnetite particles with conductive carbon black (CB; Vulcan<sup>®</sup>

XC72, Cabot Corp., USA) with a weight ratio of 9:1, along with binder (PTFE, 2 wt %). The entire mixture was spread onto Ti meshes, which served as current collectors. All electrodes had an active area of  $1 \text{ cm}^2$  and a thickness of  $750 \mu\text{m}$ . The electrolytes under study were aqueous solutions containing  $1 \text{ M Na}_2\text{SO}_3$ ,  $\text{KOH}$  and  $\text{Na}_2\text{SO}_4$ , respectively.

Electrochemical characterizations were carried out with an either two- or three-electrode configuration at room temperature on an electrochemical analyser (Eco Chemie PGSTAT30). All electrochemical characterizations except for the open-circuit decay study were carried out based on the two-electrode configuration, which comprised two plane-type electrodes of the same composition. The open-circuit decay study, on the other hand, was conducted with the three-electrode configuration, which additionally adopted a reference electrode of  $\text{Ag}/\text{AgCl}/\text{saturated KCl}$  (EG&G,  $197 \text{ mV}$  vs NHE at  $25 \text{ }^\circ\text{C}$ ). The specific leakage current ( $\text{mA F}^{-1}$ ) was expressed in terms of the leakage current ( $\text{mA}$ ) of an electrode divided by its capacitance ( $\text{F}$ ). The BET surface area was determined from nitrogen adsorption (ASAP2000, Micromeritics). The bulk chemical analyses of the particles were analyzed by XRD on a MacScience/MXP diffractometer with  $\text{CuK}_\alpha$  radiation.

### 3. Results and discussion

Figure 1 compares the voltammograms acquired from the three aqueous electrolytes. As mentioned earlier,  $\text{Na}_2\text{SO}_3$  gave the largest capacitance, while  $\text{Na}_2\text{SO}_4$  resulted in the smallest. Chronopotential analysis [18] under a constant current of  $15 \text{ mA g}^{-1}$  showed specific capacitances of  $27.0$ ,  $5.7$  and  $5.3 \text{ F (g-Fe}_3\text{O}_4)^{-1}$  for  $\text{Na}_2\text{SO}_3$ ,  $\text{KOH}$ , and  $\text{Na}_2\text{SO}_4$ , respectively. Contributions from the CB component were accessed from blank CB electrodes (without magnetite) and subtracted. It was noticed that the BET surface area

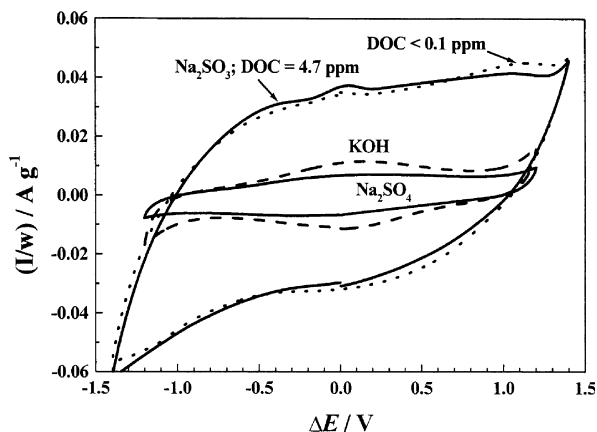


Fig. 1. Cell voltammograms for magnetite supercapacitors employing aqueous electrolytes of  $1 \text{ M Na}_2\text{SO}_3$  with a DOC of either  $4.7$  or  $< 0.1 \text{ ppm}$ ,  $\text{KOH}$ , and  $\text{Na}_2\text{SO}_4$ , respectively. Letter w of the x-axis represents weight of active materials, including magnetite and carbon black, in one electrode. Voltage sweep rate  $2 \text{ mV s}^{-1}$ .

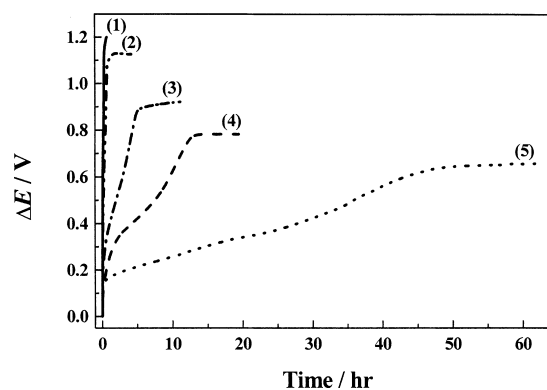


Fig. 2. Chrono-potentiometric curves under constant-current charging for the cell comprising  $1 \text{ M Na}_2\text{SO}_3$  electrolyte. Key: (1) 1, (2) 0.5, (3) 0.1, (4) 0.05 and (5)  $0.01 \text{ mA cm}^{-2}$ .

of the magnetite particles is  $34 \text{ m}^2 \text{ g}^{-1}$  and this is translated to a surface specific capacitance of about  $80 \mu\text{F cm}^{-2}$  in  $1 \text{ M Na}_2\text{SO}_3$ , almost ten times that reported for carbon [20].

Upon being charged under constant current, the capacitor cell showed a monotonic potential increase up to a 'steady-state' potential where the imposed current became equal to the leakage current, as shown in Figure 2 for the case of  $1 \text{ M Na}_2\text{SO}_3$ . When the leakage current was plotted against the steady-state potential (Figure 3), it was found that the current increased dramatically as the cell potential exceeds certain limit, which depends on the electrolyte. The sudden increase in leakage current signals the occurrence of extensive faradaic reactions and hence sets the practical operating potential limit. Accordingly, the operating potential range are about  $1.0$  and  $1.1 \text{ V}$  for  $1 \text{ M KOH}$  and  $\text{Na}_2\text{SO}_3$ , respectively (Figure 3). That of  $\text{Na}_2\text{SO}_4$  is greater than  $1.2 \text{ V}$ . Below these potential limits, the leakage currents were less than  $0.1 \text{ mA F}^{-1}$ .

Although the dissolved oxygen content (DOC) had little effect on the magnitude of capacitance (Figure 1), it was found to have a rather profound effect on the leakage current properties. The DOC of the electrolytes

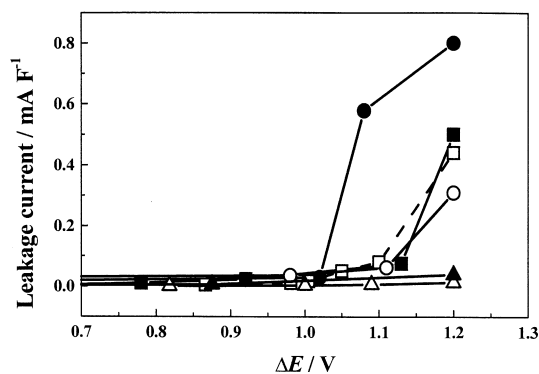


Fig. 3. Leakage current as a function of applied voltage for measurements under either an open-air environment (solid symbols) or an evacuated condition with  $\text{DOC} < 0.1 \text{ ppm}$  (open symbols) for different electrolytes. Key: (■, □)  $\text{Na}_2\text{SO}_3$ ; (●, ○)  $\text{KOH}$ ; (▲, △)  $\text{Na}_2\text{SO}_4$ .

in an open-air environment was 4.7 ppm and was reduced to be less than 0.1 ppm by first bubbling electrolytes with nitrogen and then carrying out the entire characterization experiments with the capacitor cell evacuated and sealed. In general, reducing DOC was found to reduce the leakage current (Figure 3). For  $\text{KOH}_{\text{aq}}$ , in particular, this enlarged the operating potential range from 1.0 V to 1.1 V (Figure 3).

The self-discharge behaviours of the electrode were characterized by recording chrono-potentiometric curves on open-circuit after the electrode was charged to certain potentials. It was found that, when the decaying potentials were plotted against the logarithm of time,  $\log(t)$ , all these electrolytes gave basically the same decay behaviour (Figure 4). That is, the decaying potentials can be fitted against  $\log(t)$  by two straight lines preferably within different time regions, and the slopes in these regions are almost the same for different electrolytes (Figure 4). The self-discharge behaviours of the oxide electrode, however, are definitely different from that of CB, of which the decaying potentials do not correlate linearly with  $\log(t)$  (Figure 4). Conway et al. discussed three possible self-discharge mechanisms for electrochemical capacitors and batteries, including activation- and diffusion-controlled faradaic processes and internal ohmic leakage, and derived different potential against time relationships [21, 22]. The linear dependence of decay potential against  $\log(t)$  can be accounted for by the self-discharge mechanism involving an activation-controlled interfacial faradaic reaction that follows the Tafel equation. In this mechanism, the slope of the correlating line is the negative of the Tafel slope of the initial polarization process,  $RT/\alpha F$ . The fact that the same slope is observed for all the electrolytes may indicate the same self-discharge reaction mechanism taking place. On the other hand, the change in slope with time indicates a change in the reaction mechanism. It was noted that the transition between the two linear regions for the oxide electrode (containing 10 wt % CB) occurred at about the same time (between 10 and 100 s) when there is a rapid drop in potential observed for the pure CB electrode. It is likely that the change in the correlating slope is due to the presence of the CB

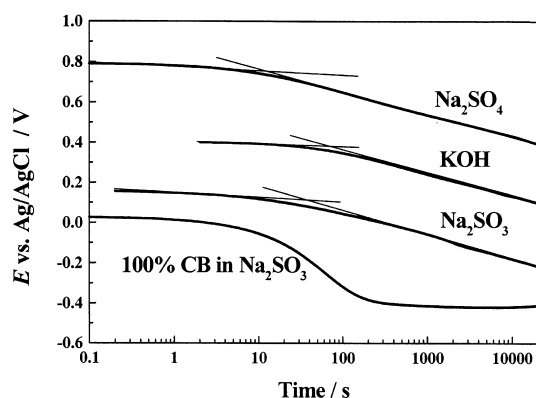


Fig. 4. Open-circuit potential decay following charging.

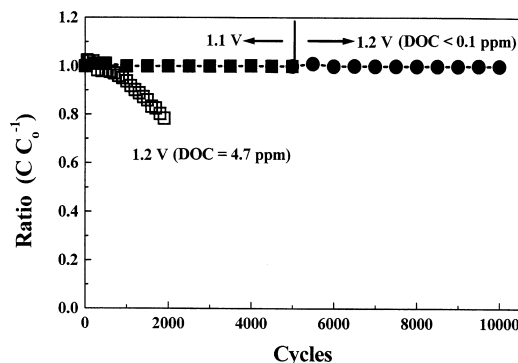


Fig. 5. Cycling stability ( $C$  is the capacitance and  $C_0$  is the initial capacitance after the first cycle). Electrolyte 1 M  $\text{Na}_2\text{SO}_3(\text{aq})$ ; cycling voltage 1.1 or 1.2 V as indicated.

component and that the self-discharge reaction at the CB surface dominates the initial self-discharge process while that at the oxide surface prevails later.

Study of the cycling stability was carried out only on the sulfite electrolyte as it gave the largest capacitance and hence has the greatest application potential. It was found that the stability was again markedly affected by DOC. When cycled within the range 0 to 1.2 V in an open-air environment, the capacitance dropped by 22% after 2000 cycles (Figure 5). In contrast, with a DOC less than 0.1 ppm, the capacitance of the electrode remained essentially unchanged after ten thousand cycles over a time span of nearly three months with a cycling range of either 1.1 or 1.2 V (Figure 5).

In summary, while the capacitance of the magnetite supercapacitor depends heavily on the electrolytes, including solutions of  $\text{Na}_2\text{SO}_3$ ,  $\text{KOH}$  and  $\text{Na}_2\text{SO}_4$ , the self-discharge process in these electrolytes appear to be the same. On the other hand, dissolved oxygen in the electrolyte has a profound effect on the leakage current and cycling stability. Reduction in DOC reduces leakage current and significantly improves the cycling stability. In particular,  $\text{Na}_2\text{SO}_3(\text{aq})$  gives a capacitance of nearly  $30 \text{ F (g-Fe}_3\text{O}_4)^{-1}$  or  $80 \mu\text{F cm}^{-2}$  of actual surface area, and the electrode showed no deterioration after  $10^4$  cycles with a DOC less than 0.1 ppm.

## Acknowledgement

The work is partly supported by the National Science Council of Republic of China under contract NSC 90-2214-E-002-009.

## References

1. B.E. Conway, *J. Electrochem. Soc.* **138** (1991) 1539.
2. S. Sarangapani, B.V. Tilak and C.-P. Chen, *J. Electrochem. Soc.* **143** (1996) 3791.
3. D.C. Grahame, *Chem. Rev.* **41** (1947) 441.
4. M.A.V. DeVanathan and B.V.K.S.R.A. Tilak, *Chem. Rev.* **65** (1965) 635.

5. S. Trasatti and G. Buzzanca, *J. Electroanal. Chem. Interf. Electrochem.* **29** (1971), App. 1.
6. L.D. Burke, O.J. Murphy, J.F. O'Neill and S. Venkatesan, *J. Chem. Soc. Faraday Trans. Part I* **73** (1977) 1659.
7. B.E. Conway, V. Birss and J. Wojtowicz, *J. Power Sources* **66** (1997) 1.
8. J.P. Zheng and T.R. Jow, *J. Electrochem. Soc.* **142** (1995) L6.
9. J.W. Ling, K.E. Swider, C.I. Merzbacher and D.R. Rolison, *Langmuir* **15** (1999) 780.
10. V. Srinivasan and J.W. Weidner, *J. Electrochem. Soc.* **144** (1997) L210.
11. J. Mozota and B.E. Conway, *Electrochim. Acta* **28** (1982) 1.
12. T.C. Liu, G. Pell and B.E. Conway, *J. Electrochem. Soc.* **145** (1998) 1882.
13. M. Waidhas and K. Mund, in F.M. Delnirk, D. Ingersoll, X. Andrieu and K. Naoi (Eds), Proceedings of the Symposium on 'Electrochemical Capacitors II', The Electrochemical Society, Pennington, NJ (1996), p. 180.
14. S. Trasatti and D. Kurzweil, *Platinum Metal Rev.* **38** (1994) 46.
15. J.P. Zheng and T.R. Zheng, *J. Electrochem. Soc.* **145** (1998) 49.
16. H.Y. Lee and J.B. Goodenough, *J. Solid State Chem.* **144** (1999) 220.
17. H.Y. Lee and J.B. Goodenough, *J. Solid State Chem.* **148** (1999) 81.
18. N.L. Wu, Y.P. Lan, C.Y. Han, S.Y. Wang and L.R. Shiue, Proceedings of 201st Meeting of American Electrochemical Society, Philadelphia, PA, 12–17 May (2002).
19. Tsouris, DePaoli and J.T. Shor, *US Patent 6 179 987 B1* (2001).
20. D. Qu and H. Shi, *J. Power Sources* **74** (1998) 99.
21. B.E. Conway, W.G. Pell and T.C. Liu, *J. Power Sources* **65** (1997) 53.
22. T.C. Liu, W.G. Pell and B.E. Conway, *Electrochim. Acta* **42** (1997) 3541.